Pragya Darshan 2023, 5(2): 63-70
ISSN: 2542-2634 (print)

@DEPAN, UCU
Research Article

Anion Exchange Membrane Functionalized by Phenol-formaldehyde Resins: Functional Group, Morphology, and Absorption Analysis

D. Parajuli[1], *, N. Murali[2], K. Samatha[3], N. L. Sahu[4] and B. R. Sharma[5]

[1]Research Center for Applied Science and Technology, Tribhuvan University, Nepal
[2]Department of Engineering Physics, AUCE (A), Andhra University, Visakhapatnam, India
[3]Department of Physics, AUCST, Andhra University, Visakhapatnam, India
[4]Department of Physics, Tri-Chandra Multiple Campus, Kathmandu, Nepal
[5]Department of Physics, Janapriya Multiple Campus, Pokhara, Kaski
* Email: deepenparaj@gmail.com

Received: 7th May, 2023; Revised: 7th July, 2023; Accepted: 7th August, 2023

Abstract: We have developed a straightforward and uncomplicated technique for creating alkaline exchange membranes (AEMs) that possess both high alkaline durability and improved ionic conductivity. This method provides an appealing alternative to conventional approaches, notably by eliminating the need for the use of the carcinogenic reagent chloromethyl methyl ether, typically employed in AEM preparation. Examination of the membranes via scanning electron microscopy (SEM) reveals a consistently smooth surface. Augmenting the ion-exchange material's weight percentage in the casting solution results in enhanced water content, ion exchange capacity, and electrical conductivity. Importantly, our approach entirely circumvents the use of the hazardous chloromethyl methyl ether reagent, commonly associated with AEM preparation. TGA for thermal stability and chemical stability, conductivity with impedance data, and electrochemical tests are going on. The outcomes of this study present an appealing alternative to traditional methods for AEM synthesis.

Keywords: *AEM, Phenol-formaldehyde, FTIR, SEM, water absorption*.

Introduction

Polymer electrolyte membrane fuel cells and rechargeable batteries (D. Parajuli, Murali, Samatha, & Veeraiah, 2022; D. Parajuli, Taddesse, Murali, Veeraiah, et al., 2022) are recognized as modern, environmentally friendly energy conversion and storage technologies due to their exceptional energy conversion efficiency (Gu et al., 2015; D. Parajuli, Bhandari, et al., 2023; D. Parajuli, Kc, et al., 2023; D. Parajuli, Gaudel, et al., 2023; D Parajuli, Kumar Shah, Kc, Kumar, et al., 2022; Shah et al., 2022), minimal local pollution, low noise levels, and cost-effective maintenance. In recent years, considerable research has focused on anion-exchange membranes (AEMs) as separators in these devices. AEMs hold the potential to address the limitations of proton exchange membrane fuel cells based on Nafion, which include low tolerance to carbon monoxide, high electrokinetic overpotentials, significant fuel permeation, and elevated catalyst costs (Feng et al., 2016; X. Lin et al., 2012; L. Liu et al., 2015; Shim & Kim, 2010; Zheng et al., 2017). Among the various methods employed for AEM synthesis, a common approach involves modifying the base polymer matrix, such as polyphenylene oxide, polyaryl ether sulfone ketones, and poly(ether ketone) (PEK) (Y. Liu et al., 2016; Tuan & Kim, 2016). Typically, ion-exchange groups are introduced into these membranes through a process involving chloromethylation of the polymers, followed by exposure to trimethylamine (TMA) to create the corresponding trimethyl-type quaternary ammonium (QA) head group (Tuan & Kim, 2016). However, QA groups are susceptible to Hoffmann degradation reactions in strong alkaline environments, compromising the durability of these membranes (Ran et al., 2017). Additionally, AEMs produced using these methods often exhibit inadequate ionic conductivity, rendering them unsuitable for practical applications (Merle et al., 2011). Consequently, significant research efforts have been directed toward developing membranes that combine excellent chemical stability, high ionic conductivity, and robust mechanical strength (Maurya et al., 2015). Researchers like X. Lin et al. and C. Qu et al. have successfully developed a series of AEMs featuring pendant guanidinium groups, which offer improved alkaline stability and enhanced ionic conductivity. These enhancements in the properties of guanidinium-functionalized AEMs stem from the high basicity and resonance-stabilized structure of the guanidinium functional groups (X. Lin et al., 2012; Qu et al., 2012). Notably, the pKa of guanidine in aqueous environments is 13.6, signifying its exceptional alkalinity and resulting in a higher concentration of mobile hydroxide ions compared to trimethylamine (Ishikawa, 2009; Zhang et al., 2010).

In 1872 Von Bayer reported the formation of the first synthetic resin by polycondensation of phenol and formaldehyde. In 1910 Baekeland made the first plastic by the polycondensation of phenol and formaldehyde (Brydson, 1999). The ion exchange property of PF resin was discovered by Adams and Holmes in 1935 (Inamuddin & Luqman, 2012). Around 1940, synthetic ion-exchange membranes based on phenol-formaldehyde condensation products were used in many industrial applications such as electrodialysis, electrodialytic concentration of seawater, and desalination of saline water (Alexandratos, 2008; Brydson, 1999; Sata, 2002; Y. Wang & Xu, 2013). Polycondensation of sodium phenol sulfonate, phenol, and formaldehyde was carried out in the presence of an alkali catalyst for the preparation of ion exchange resins. Low molecular weight prepolymer was coated on a reinforcing fabric such as glass fiber and cured to complete the condensation reaction. Anion-exchange membranes were also prepared by polycondensation of phenylenediamines, phenol, and formaldehyde. The durability of such membranes was not

sufficient for long-term usage (Alexandratos, 2008; Sata, 2002; Y. Wang & Xu, 2013).

In the last two decades, remarkable progress has been made in the development of high-performance polymers as matrices for membranes. Due to high mechanical strength, good chemical resistance, solubility in common solvents, and commercial availability, PVC polymers are widely used for the preparation of polymer membranes. PVC-based membranes are commercially employed as battery separators, ultra-filtration membranes, and matrices in proton exchange membranes (PEM) for fuels (Allan et al., 2015; An et al., 2003; Maghsoud et al., 2017). J.W. Qian and et al. reported good performance for pervaporation of benzene/cyclohexane mixtures using blend membranes of PVC and EVA (An et al., 2003).

Sulfonated PVC membranes with high permeability and selectivity were developed as proton exchange membranes for fuel cells (Allan et al., 2015). PVC blend membranes with high antifouling properties are fabricated by incorporating a novel zwitter ionic polymer into the PVC matrix (Fang et al., 2017). Yongsheng Chen et al. fabricated PVC/Fe_2O_3 ultra filtration membranes with good performance (Demirel et al., 2017). Y. Jafarzadeh et al. developed PVC/PC blend membranes for ultrafiltration (Behboudi et al., 2017). Recently, we have studied some energy efficient devices made of ferrites and MXenes (D. Parajuli, Murali, & Samatha, 2022; D. Parajuli, Murali, K. C, Karki, et al., 2022; D. Parajuli, Murali, Rao, Ramakrishna, et al., 2022; D. Parajuli, Taddesse, Murali, & Samatha, 2022; D. Parajuli, Uppugalla, et al., 2023; D. Parajuli, Vagolu, Chandramoli, Murali, et al., 2022; D Parajuli, Murali, et al., 2021; D Parajuli, Vagolu, et al., 2021; Deependra Parajuli & Samatha, 2021, 2022).

The present work deals with the development of anion-exchange resins by chemical functionalization of phenol-formaldehyde resins with guanidinium groups as a continuation of our previous work (D. Parajuli, Murali, et al., 2023). First phenol and formaldehyde were condensed in the basic medium and the resins obtained were condensed with guanidine hydrochloride in the presence of formaldehyde in the basic medium resulting in the formation of cross-linked polymers. The membranes were made by homogenizing ion-exchange resins and a binder polymer such as PVC in an appropriate solvent such as tetrahydrofuran (THF) followed by solution casting.

Experimental

Materials

Phenol, formaldehyde solution (37%), tetrahydrofuran (THF), guanidine hydrochloride, and ammonia solution were purchased from Merck. Commercial-grade PVC of high molecular weight was used.

Synthesis of anion–exchange material

Phenol and formaldehyde (40%) in the molar ratio of 1:2 were refluxed in a basic medium (pH 9) till a yellow resin was separated from the above reaction mixture. It was taken out, washed with D.I. water, and dried. The resin was finely powdered and dispersed in acetone and heated with 1-mole guanidine chloride solution for 2 h at 80°C. The final condensation product was separated from the reaction mixture, washed with water, filtered, and dried.

Preparation of anion–exchange membrane

A heterogeneous anion-exchange membrane was prepared by the solution casting method. Definite weight of anion–exchange material and PVC powder were stirred in an appropriate solvent such as tetrahydrofuran (THF) for about 8h at room temperature. The homogeneous suspension was cast onto a clean glass plate using a film applicator. Composite membranes were peeled from the glass plate after 48 h. The composite membranes were 80 µm thick. All the membranes were immersed in 2M NaOH solution for 24 h prior to testing. The compositions of the membranes were varied by using different amounts of guanidine functionalized anion-exchange material (10 wt%, 20 wt%, 30 wt%, and 40 wt %). The corresponding membranes are represented as P1, P2, P3 and P4.

Characterization Techniques

The membranes were characterized by FTIR spectroscopy using the Perkin-Elmer spectrum (Model L160000A) over a range of 4000 - 400 cm^{-1}. The surface morphologies of the composite membranes were examined by a scanning electron microscope (JSM-5600, JEOL Co., Japan) as in our previous works (D. Parajuli, Taddesse, Murali, & Samatha, 2022a)(D. Parajuli, Raghavendra, et al., 2021)(D. Parajuli, Devendra, et al., 2021)(D. Parajuli, Taddesse, Murali, & Samatha, 2022b)(Deependra Parajuli & Samatha, 2022)(D. Parajuli, Murali, Raghavendra, et al., 2023)(D. Parajuli, Dangi, Sharma, et al., 2023). The samples were coated with a thin layer of gold by ion sputtering prior to microscopic examination. The SEM images of the anion-exchange membranes were transformed into a computer and evaluated with an image analysis system. In these experiments, we analyzed thin films with an average mass of 15 mg. The procedure involved heating the samples from room temperature to 850°C while maintaining a nitrogen atmosphere, with a heating rate of 10°C per minute (Di Vona et al., 2014). For assessing the water uptake of these composite membranes, we employed the following methodology. First, the membranes were soaked in distilled water at room temperature for a duration of 24 hours to ensure they reached a state of equilibrium with the surrounding moisture. Subsequently, we meticulously removed any excess surface water from the membranes by gently wiping them with filter paper, immediately followed by recording their weight. To obtain accurate measurements, the samples were then subjected to vacuum drying for a period of two days and subsequently weighed once more.

The water uptake was calculated as follows.

$$Water\ intake\ (\%) = \frac{W_{wet} - W_{dry}}{W_{dry}} \times 100\% \quad (3)$$

The ion exchange capacities (IECs) of the composite membranes were assessed using the double titration method. To calculate IECs, the following procedure was followed: Accurately weigh the samples, denoting the mass of the water-swollen membrane as Wwet and the mass of the dry membrane as Wdry. Immerse these weighed samples in 25 ml of a 0.05 M HCl solution for a duration of 48 hours. Back-titrate the HCl solution with a 0.05 M NaOH solution while employing phenolphthalein as an indicator. The IECs of the samples can then be calculated using the appropriate equation.

$$IEC = \frac{\eta_1 - \eta_2}{M_{dry}} \quad (2)$$

The ion exchange capacity (IEC) calculation process involves the following steps: n_1 and n_2 are determined, which represent the quantities of hydrochloric acid (in millimoles, mmol) required before and after reaching equilibrium, respectively. Measure the mass of the dried sample (M_{dry}, in grams). Apply the provided equation to compute the IEC value for each sample. Repeat these calculations for all three samples, and then derive the average value from these outcomes to establish the membrane's IEC value. To assess the ionic conductivity of the membranes, electrochemical impedance spectroscopy (EIS) techniques were utilized. These assessments were carried out using the AUTOLAB 50519 PGSTAT instrument.

To perform these measurements, fully hydrated membranes were positioned in the conductivity cell, which was subsequently filled with a 1M NaOH solution. The total resistance of the system, including both the membrane and the solution, was recorded (R_{total}). The resistance of the solution alone was measured separately, excluding the presence of the membrane (referred to as $R_{solution}$). The membrane's resistance (R_{mem}) was then determined by subtracting Rsolution from Rtotal. For accurate measurements, the thickness of the membrane was gauged using a digital micrometer. This measurement was carried out by placing the membrane between two glass slides, ensuring a flat surface and minimal compression. Subsequently, the hydroxide conductivity (σ) of the membrane was calculated using the following formula: σ = L/RA (in mS cm-1), where σ represents the hydroxide conductivity, R is the ohmic resistance of the membrane (in ohms, Ω), L is the thickness of the membrane (in centimeters, cm), and A is the cross-sectional area of the membrane sample (in square centimeters, cm^2).

Methanol permeability through the membrane was determined using a custom-made apparatus, employing the Gasa method (Gasa et al., 2007), which is based on a permeation cell design adapted from Walker et al. (Walker et al., 1999). The procedure involved sealing a precise amount of methanol within a permeation cell and allowing it to diffuse through a hole with an area of 4 cm2, covered by the membrane. These measurements were carried out at room temperature. Essentially, the permeation process entails the dissolution and diffusion of methanol molecules within the membrane material. The mass of methanol contained in the vial was monitored over time, and the membrane's permeability (P) was calculated using the following equation:

$$P = \frac{N \times l}{V.P. \times A \times t}$$

Here, N: The number of moles of methanol lost (in moles), l: The thickness of the membrane, V.P.: The saturated vapor pressure of methanol at 25°C, A: The membrane area available for methanol permeation (in square centimeters, cm^2), t: The time during which the measurement was conducted (in days).

To assess the alkaline stability, a 2M aqueous sodium hydroxide (NaOH) solution at room temperature was used. In this test, the composite membrane sample was submerged in the 2M NaOH solution for a duration of 2 weeks. Afterward, the membranes were removed, rinsed with deionized (D.I.) water, wiped with tissue paper, and then subjected to FTIR analysis to detect any degradation or alterations in chemical structure. Additionally, the loss of weight of the membrane was measured (X. Lin et al., 2012)(B. Lin et al., 2010)[4, 28]. For evaluating oxidative stability, the samples, each measuring 3cm x 3cm, were immersed in Fenton's reagent, which consists of 30 ppm FeSO4 in 30% H_2O_2. This immersion took place for 24 hours at 25°C, and the weight loss of the membrane was monitored over time (T. Wang et al., 2012).

All-iron flow battery experiments

The experiments involving the all-iron flow battery were conducted within a flow cell hardware configuration, where electrolytes flowed between two electrodes, separated by the previously prepared membrane (Manohar et al., 2016). All experiments were consistently performed with electrolyte flow rates set at 25 milliliters per minute (ml min-1). The electrolytes used for both the positive and negative electrodes consisted of 1M FeCl2 and 1.5M NH4Cl. The electrodes themselves were constructed from graphite plates, each having a cross-sectional area of 16 square centimeters (cm^2). To determine the charging efficiency of the all-iron redox flow cell, a specific procedure was followed. The cell was initially charged at a rate of 100 milliamperes per square centimeter (mA cm-2) for a duration of 100 seconds. Subsequently, it was discharged at a rate of 50 mA cm-2, with these operations being performed using the AUTOLAB 50519 PGSTAT instrument. The performance of the cell was assessed based on its columbic efficiency (CE), which is calculated as the ratio of the cell's discharge capacity (Qdis) to its charge capacity (Qch).

Results and Discussion

Functional group analysis

Fig. 1(a-e) shows the FT-IR spectra of (a) Guanidinium chloride (b) Anion-exchange material (c) PVC membrane (d) Membrane P2 (e) MembraneP4 respectively. The spectrum (a) of Guanidinium chloride shows broadband in the region 3100-3400 cm-1, due to the stretching vibration of N-H bonds of guanidinium (Sajjad et al., 2015). The peak at 1654 cm-1 is attributed to the coupled vibrations of N-H in-plane bending vibrations and asymmetric stretching vibrations of the C-N group of the guanidinium group. The peak at 1198 cm-1 is assigned to the N-H bending vibration of the guanidinium group (Antony et al., 2009; Braiman et al., 1999).

The spectrum (b) of anion-exchange material shows the band in the region 3100-3400 cm-1 attributed to the stretching vibrations of N-H groups and O-H stretching vibrations. The absorption peak in the region of 3100-3400 cm-1 of the anion-exchange material is weaker, which indicates that the majority of functional groups such as –NH2 offered by guanidine and –OH group of phenol were subjected to condensation reaction with formaldehyde. The peak at 1654 cm-1 is a coupled vibration having contributions from both N-H in-plane bending vibrations and asymmetric stretching vibrations of C-N groups of guanidinium ion. The absorption peaks at 1504 cm-1 are attributed to the vibration of the aromatic ring of benzene in phenol. The peak at 1078 cm-1 is assigned to C-O-C ether links formed during condensation reactions with formaldehyde. The spectrum (c) of PVC membrane shows strong signals at 1425 cm-1, 1340 cm-1, 1200 cm-1, 1050 cm-1, 950 cm-

1 and at 690 cm-1. These correspond to the C-C, C-H, and C-Cl vibrations found within the PVC polymer. The peak at 1600 cm-1, and 1505 cm-1 is due to C-C aromatic stretching vibrations of the phenyl group (Poljanšek & Krajnc, 2005; Yanshan et al., 2014). The spectra (d), and (e) correspond to that of the membranes (P2 and P4) with increasing amounts of anion-exchange material. The spectra (d,e) of the membranes show peaks in the region of 3000-3400cm-1 corresponding to the stretching vibrations of N-H groups of guanidine and stretching vibrations of O-H groups. The band at 2917 cm-1 could be assigned to stretching vibrations of C-H group groups of the polymer backbone and the band at 1450 cm-1 is attributed to bending vibrations of the -CH2 group (Yanshan et al., 2014). The peaks at 1600 cm-1 and 1505 cm-1 correspond to the C-C aromatic stretching vibrations of the phenyl group. The above spectral observations suggest the successful incorporation of anion-exchange material into the polymer matrix (Ma et al., 2012; Yanshan et al., 2014).

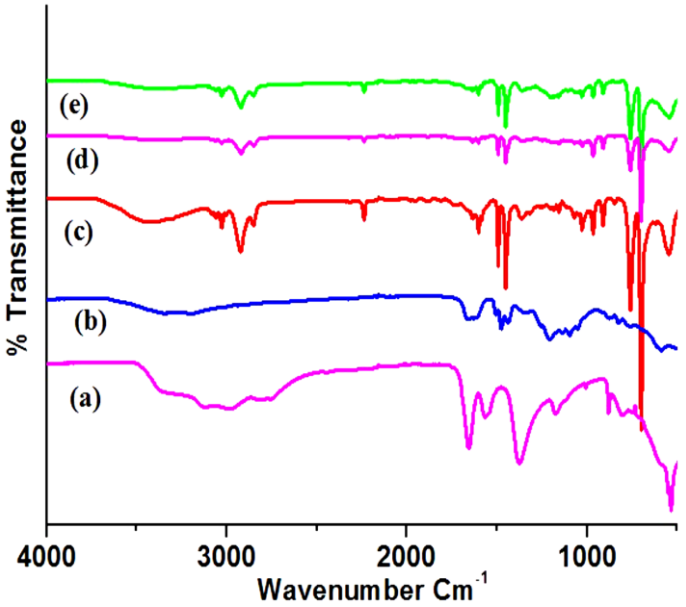

Fig. 1 FT-IR spectrum of (a) Guanidinium chloride (b) anion-exchange material (c) PVC polymer (d) Ion-exchange membrane P2 (e) Ion-exchange membrane P4

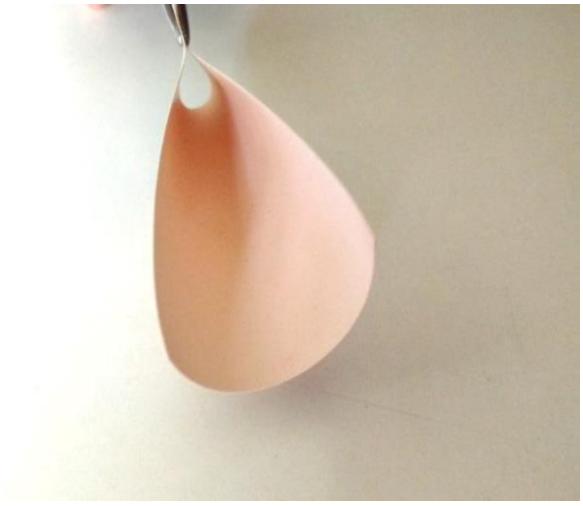

Fig. 2 Photograph of the prepared Ion-exchange membrane P4

SEM analysis

Scanning electron microscopy (SEM) is used to investigate the microstructures of the membranes. Fig. 3 (smooth and defect-free surface of the membrane without any cracks or pinholes, indicating the fine quality of the membrane. of composite membrane P4 using 40% anion exchange magnifications and a) shows the SEM image of PVC membrane which presents a Fig. 3 (b-c) shows the surface morphology using 40% anion exchange material at different anion-exchange material. However, Fig. 3(d) shows the cross membrane P4 found to be flexible as shown in the photograph (a) PVC membrane (b & c) composite material at different magnifications (d) cross-sectional image of membrane P4. The P4 Fig. 2. a) shows the SEM image of the PVC membrane which presents Fig. 3 (b-c) shows the surface morphology using 40% anion exchange material at different anion-exchange materials. However, Fig. 3(d) shows the cross membrane P4 found to be flexible as shown in the photograph (a) PVC membrane (b & c) composite material at different magnifications (d) cross-sectional image of membrane P4.

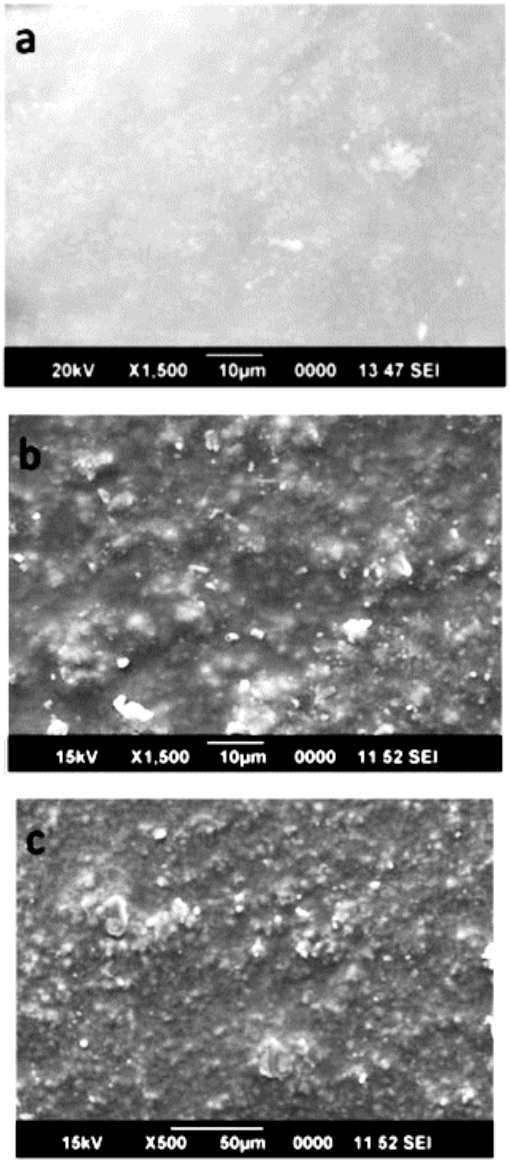

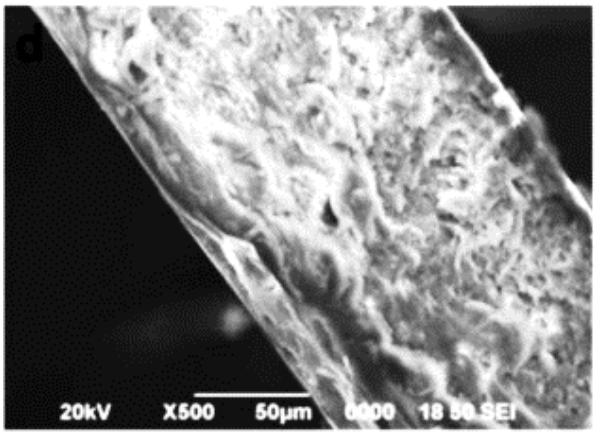

Fig. 3 SEM images of membranes: (a) PVC membrane (b&c) composite membrane P4, using 40% anion exchange magnifications and (d) cross-sectional image of membrane P4.

Water uptake

The water uptake values of the membranes with different contents of anion-exchange material are shown in Fig.4. Water uptake of AEM is a key factor that determines the performance of electrochemical devices. Higher water uptake values will facilitate hydroxide transport by generating solvated ionic species and broadening ion transport channels, to maintain the high ionic conductivity of the materials (Merle et al., 2011). Water uptake primarily depends on the microstructure of the membrane and functional groups of ion exchange groups attached to the polymer chains. The water uptake of these membranes increased moderately with an increase in the content of ion exchange material. This indicates that the water uptake strongly depends on the amount of ion-exchange material. However, excessive water uptake may lead to the deterioration of the AEM's mechanical properties. An ideal AEM should exhibit proper water uptake, high conductivity, and excellent mechanical properties. In these membranes, the guanidinium ion exchange group is also thought to participate in absorbing water due to hydrogen bonding capacity.

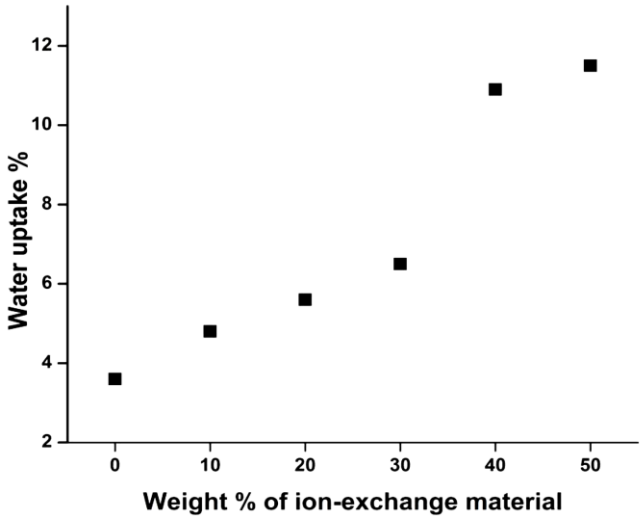

Fig. 4 Water uptake of membranes with varying anion-exchange material content

Conclusions

We developed a simple and facile method to prepare AEMs with high alkaline stability and enhanced ionic conductivity. The facile nature of the technique offers an attractive alternative to traditional approaches. This method avoids the use of chloromethyl methyl ether, the carcinogenic reagent generally used for AEM preparation. SEM images of membranes showed a relatively uniform surface for the membranes. The increase of ion-exchange material wt% in the casting solution led to an improvement in water content, Ion exchange capacity, and electrical conductivity. This method completely avoids carcinogenic and toxic reagent chloromethyl methyl ether commonly used for AEM preparation. The results of this study offer an attractive alternative to the traditional approaches for the synthesis of AEMs.

References:

Alexandratos, S. D. (2008). Ion-Exchange Resins: A Retrospective from Industrial and Engineering Chemistry Research. *Industrial and Engineering Chemistry Research*, *48*(1), 388–398. https://doi.org/10.1021/IE801242V

Allan, J. T. S., Prest, L. E., & Easton, E. B. (2015). The sulfonation of polyvinyl chloride: Synthesis and characterization for proton conducting membrane applications. *Journal of Membrane Science*, *489*, 175–182. https://doi.org/10.1016/J.MEMSCI.2015.03.093

An, Q. F., Qian, J. W., Sun, H. B., Wang, L. N., Zhang, L., & Chen, H. L. (2003). Compatibility of PVC/EVA blends and the pervaporation of their blend membranes for benzene/cyclohexane mixtures. *Journal of Membrane Science*, *222*(1–2), 113–122. https://doi.org/10.1016/S0376-7388(03)00260-6

Antony, C. J., Bushiri, M. J., Varghese, H. T., Panicker, C. Y., & Fleck, M. (2009). Spectroscopic properties of guanidinium zinc sulphate [C(NH2)3]2Zn(SO4)2 and ab initio calculations of [C(NH2)3]2 and HC(NH2)3. *Spectrochimica Acta Part A: Molecular and Biomolecular Spectroscopy*, *73*(5), 942–945. https://doi.org/10.1016/J.SAA.2009.04.024

Behboudi, A., Jafarzadeh, Y., & Yegani, R. (2017). Polyvinyl chloride/polycarbonate blend ultrafiltration membranes for water treatment. *Journal of Membrane Science*, *534*, 18–24. https://doi.org/10.1016/J.MEMSCI.2017.04.011

Braiman, M. S., Briercheck, D. M., & Kriger, K. M. (1999). Modeling vibrational spectra of amino acid side chains in proteins: Effects of protonation state, counterion, and solvent on arginine C-N stretch frequencies. *Journal of Physical Chemistry B*, *103*(22), 4744–4750. https://doi.org/10.1021/JP983011B/SUPPL_FILE/JP983011B_S.PDF

Brydson, J. A. (1999). *Plastics materials*. 920. https://archive.org/details/0347-pdf-brydson-plastics-materials-7e-butterworth-1999

Demirel, E., Zhang, B., Papakyriakou, M., Xia, S., & Chen, Y. (2017). Fe2O3 nanocomposite PVC membrane with enhanced properties and separation performance. *Journal of Membrane Science*, *529*, 170–184.

https://doi.org/10.1016/J.MEMSCI.2017.01.051

Di Vona, M. L., Narducci, R., Pasquini, L., Pelzer, K., & Knauth, P. (2014). Anion-conducting ionomers: Study of type of functionalizing amine and macromolecular cross-linking. *International Journal of Hydrogen Energy*, *39*(26), 14039–14049. https://doi.org/10.1016/J.IJHYDENE.2014.06.166

Fang, L. F., Jeon, S., Kakihana, Y., Kakehi, J. ichi, Zhu, B. K., Matsuyama, H., & Zhao, S. (2017). Improved antifouling properties of polyvinyl chloride blend membranes by novel phosphate based-zwitterionic polymer additive. *Journal of Membrane Science*, *528*, 326–335. https://doi.org/10.1016/J.MEMSCI.2017.01.044

Feng, T., Lin, B., Zhang, S., Yuan, N., Chu, F., Hickner, M. A., Wang, C., Zhu, L., & Ding, J. (2016). Imidazolium-based organic–inorganic hybrid anion exchange membranes for fuel cell applications. *Journal of Membrane Science*, *508*, 7–14. https://doi.org/10.1016/J.MEMSCI.2016.02.019

Gasa, J. V., Weiss, R. A., & Shaw, M. T. (2007). Ionic crosslinking of ionomer polymer electrolyte membranes using barium cations. *Journal of Membrane Science*, *304*(1–2), 173–180. https://doi.org/10.1016/J.MEMSCI.2007.07.031

Gu, C., Huang, N., Chen, Y., Qin, L., Xu, H., Zhang, S., Li, F., Ma, Y., & Jiang, D. (2015). π-Conjugated Microporous Polymer Films: Designed Synthesis, Conducting Properties, and Photoenergy Conversions. *Angewandte Chemie International Edition*, *54*(46), 13594–13598. https://doi.org/10.1002/anie.201506570

Inamuddin, & Luqman, M. (2012). Ion exchange technology I: Theory and materials. *Ion Exchange Technology I: Theory and Materials*, 1–550. https://doi.org/10.1007/978-94-007-1700-8/COVER

Ishikawa, T. (2009). Superbases for Organic Synthesis: Guanidines, Amidines, Phosphazenes and Related Organocatalysts. *Superbases for Organic Synthesis: Guanidines, Amidines, Phosphazenes and Related Organocatalysts*, 1–326. https://doi.org/10.1002/9780470740859

Lin, B., Qiu, L., Lu, J., & Yan, F. (2010). Cross-linked alkaline ionic liquid-based polymer electrolytes for alkaline fuel cell applications. *Chemistry of Materials*, *22*(24), 6718–6725. https://doi.org/10.1021/CM102957G/ASSET/IMAGES/MEDIUM/CM-2010-02957G_0005.GIF

Lin, X., Wu, L., Liu, Y., Ong, A. L., Poynton, S. D., Varcoe, J. R., & Xu, T. (2012). Alkali resistant and conductive guanidinium-based anion-exchange membranes for alkaline polymer electrolyte fuel cells. *Journal of Power Sources*, *217*, 373–380. https://doi.org/10.1016/J.JPOWSOUR.2012.05.062

Liu, L., Tong, C., He, Y., Zhao, Y., & Lü, C. (2015). Enhanced properties of quaternized graphenes reinforced polysulfone based composite anion exchange membranes for alkaline fuel cell. *Journal of Membrane Science*, *487*, 99–108. https://doi.org/10.1016/J.MEMSCI.2015.03.077

Liu, Y., Zhang, B., Kinsinger, C. L., Yang, Y., Seifert, S., Yan, Y., Mark Maupin, C., Liberatore, M. W., & Herring, A. M. (2016). Anion exchange membranes composed of a poly(2,6-dimethyl-1,4-phenylene oxide) random copolymer functionalized with a bulky phosphonium cation. *Journal of Membrane Science*, *506*, 50–59. https://doi.org/10.1016/J.MEMSCI.2016.01.042

Ma, F., Zhao, H., Sun, L., Li, Q., Huo, L., Xia, T., Gao, S., Pang, G., Shi, Z., & Feng, S. (2012). A facile route for nitrogen-doped hollow graphitic carbon spheres with superior performance in supercapacitors. *Journal of Materials Chemistry*, *22*(27), 13464–13468. https://doi.org/10.1039/C2JM32960C

Maghsoud, Z., Pakbaz, M., Famili, M. H. N., & Madaeni, S. S. (2017). New polyvinyl chloride/thermoplastic polyurethane membranes with potential application in nanofiltration. *Journal of Membrane Science*, *541*, 271–280. https://doi.org/10.1016/J.MEMSCI.2017.07.001

Manohar, A. K., Kim, K. M., Plichta, E., Hendrickson, M., Rawlings, S., & Narayanan, S. R. (2016). A High Efficiency Iron-Chloride Redox Flow Battery for Large-Scale Energy Storage. *Journal of The Electrochemical Society*, *163*(1), A5118–A5125. https://doi.org/10.1149/2.0161601JES/XML

Maurya, S., Shin, S. H., Kim, Y., & Moon, S. H. (2015). A review on recent developments of anion exchange membranes for fuel cells and redox flow batteries. *RSC Advances*, *5*(47), 37206–37230. https://doi.org/10.1039/C5RA04741B

Merle, G., Wessling, M., & Nijmeijer, K. (2011). Anion exchange membranes for alkaline fuel cells: A review. *Journal of Membrane Science*, *377*(1–2), 1–35. https://doi.org/10.1016/J.MEMSCI.2011.04.043

Parajuli, D., Bhandari, V., K.C., D., Thapaliya, A., Subedi, A., Dhakal, A., Dangi, S., Koirala, R., & Bhatta, M. (2023). Numerical Approach of Single-Junction InGaN Solar Cell Affected by Carrier Lifetime and Temperature. *Pragya Darshan प्रज्ञा दर्शन*, *5*(1), 58–63. https://doi.org/10.3126/PDMDJ.V5I1.52309

Parajuli, D., Dangi, S., Sharma, B. R., Shah, N. L., & KC, D. (2023). Sol-gel synthesis, characterization of ZnO thin films on different substrates, and bandgap calculation by the Tauc plot method. *BIBECHANA*, *20*(2), 113–125. https://doi.org/10.3126/BIBECHANA.V20I2.54115

Parajuli, D., Devendra, K. C., Reda, T. G., Sravani, G. M., Murali, N., & Samatha, K. (2021). RHEED analysis of the oxidized M′2M″xXyene sheets by ablated plasma thrust method in pulsed laser deposition chamber. *AIP Advances*, *11*(11), 115019. https://doi.org/10.1063/5.0068659

Parajuli, D., Gaudel, G. S., Kc, D., Khattri, K. B., & Rho, W. Y. (2023). Simulation study of TiO2 single layer anti-reflection coating for GaAs solar cell. *AIP Advances*, *13*(8), 85002. https://doi.org/10.1063/5.0153197/2904980

Parajuli, D., Kc, D., Khattri, K. B., Adhikari, D. R., Gaib, R. A., & Shah, D. K. (2023). Numerical assessment of optoelectrical

properties of ZnSe–CdSe solar cell-based with ZnO antireflection coating layer. *Scientific Reports 2023 13:1*, *13*(1), 1–13. https://doi.org/10.1038/s41598-023-38906-z

Parajuli, D., Murali, N., K. C, D., Karki, B., Samatha, K., Kim, A. A., Park, M., & Pant, B. (2022). Advancements in MXene-Polymer Nanocomposites in Energy Storage and Biomedical Applications. *Polymers 2022, Vol. 14, Page 3433*, *14*(16), 3433. https://doi.org/10.3390/POLYM14163433

Parajuli, D., Murali, N., Raghavendra, V., Suryanarayana, B., Batoo, K. M., & Samatha, K. (2023). Investigation of structural, morphological and magnetic study of Ni–Cu-substituted Li0.5Fe2.5O4 ferrites. *Applied Physics A 2023 129:7*, *129*(7), 1–12. https://doi.org/10.1007/S00339-023-06772-1

Parajuli, D., Murali, N., Rao, A. V., Ramakrishna, A., S, Y. M., & Samatha, K. (2022). Structural, dc electrical resistivity and magnetic investigation of Mg, Ni, and Zn substituted Co-Cu nano spinel ferrites. *South African Journal of Chemical Engineering*, *42*, 106–114. https://doi.org/10.1016/J.SAJCE.2022.07.009

Parajuli, D., Murali, N., & Samatha, K. (2022). Correlation between the Magnetic and DC resistivity studies of Cu substituted Ni and Zn in Ni-Zn ferrites. *BIBECHANA*, *19*(1–2), 61–67. https://doi.org/10.3126/BIBECHANA.V19I1-2.46387

Parajuli, D., Murali, N., Samatha, K., Shah, N. L., & Sharma, B. R. (2023). Structural, Morphological, and Textural Properties of Coprecipitated CaTiO3 for Anion Exchange in the Electrolyzer. *Journal of Nepal Physical Society*, *9*(1), 137–142. https://doi.org/10.3126/JNPHYSSOC.V9I1.57751

Parajuli, D., Murali, N., Samatha, K., & Veeraiah, V. (2022). Thermal, structural, morphological, functional group and first cycle charge/discharge study of Co substituted LiNi1−x-0.02Mg0.02CoxO2 (x = 0.00, 0.02, 0.04, 0.06, and 0.08) cathode material for LIBs. *AIP Advances*, *12*(8), 085010. https://doi.org/10.1063/5.0096297

Parajuli, D., Raghavendra, V., Suryanarayana, B., Rao, P. A., Murali, N., Varma, P. V. S. K. P., Prasad, R. G., Ramakrishna, Y., & Chandramouli, K. (2021). Corrigendum to "Cadmium substitution effect on structural, electrical and magnetic properties of Ni-Zn nano ferrites" [Results Phys. 19 (2020) 2211-379 103487]. *Results in Physics*, *23*, 103947. https://doi.org/10.1016/J.RINP.2021.103947

Parajuli, D., Taddesse, P., Murali, N., & Samatha, K. (2022a). Correlation between the structural, magnetic, and dc resistivity properties of Co0.5M0.5-xCuxFe2O4 (M = Mg, and Zn) nano ferrites. *Applied Physics A: Materials Science and Processing*, *128*(1), 1–9. https://link.springer.com/article/10.1007/s00339-021-05211-3

Parajuli, D., Taddesse, P., Murali, N., & Samatha, K. (2022b). Study of structural, electromagnetic and dielectric properties of cadmium substituted Ni–Zn nanosized ferrites. *Journal of the Indian Chemical Society*, *99*(3), 100380. https://doi.org/10.1016/J.JICS.2022.100380

Parajuli, D., Taddesse, P., Murali, N., Veeraiah, V., & Samatha, K. (2022). Effect of Zn2+ doping on thermal, structural, morphological, functional group, and electrochemical properties of layered LiNi0.8Co0.1Mn0.1O2 cathode material. *AIP Advances*, *12*(12), 125012. https://doi.org/10.1063/5.0122976

Parajuli, D., Uppugalla, S., Murali, N., Ramakrishna, A., Suryanarayana, B., & Samatha, K. (2023). Synthesis and characterization MXene-Ferrite nanocomposites and its application for dying and shielding. *Inorganic Chemistry Communications*, *148*, 110319. https://doi.org/10.1016/J.INOCHE.2022.110319

Parajuli, D., Vagolu, V. K., Chandramoli, K., Murali, N., & Samatha, K. (2022). Electrical Properties of Cobalt Substituted NZCF and ZNCF Nanoparticles Prepared by the Soft Synthesis Method. *Journal of Nepal Physical Society*, *8*(3), 45–52. https://doi.org/10.3126/JNPHYSSOC.V8I3.50726

Parajuli, D, Kumar Shah, D., Kc, D., Kumar, S., Park, M., & Pant, B. (2022). Influence of Doping Concentration and Thickness of Regions on the Performance of InGaN Single Junction-Based Solar Cells: A Simulation Approach. *Electrochem 2022, Vol. 3, Pages 407-415*, *3*(3), 407–415. https://doi.org/10.3390/ELECTROCHEM3030028

Parajuli, D, Murali, N., & Samatha, K. (2021). Structural, Morphological, and Magnetic Properties of Nickel Substituted Cobalt Zinc Nanoferrites at Different Sintering Temperature. *Journal of Nepal Physical Society*, *7*(2), 24–32. https://doi.org/10.3126/JNPHYSSOC.V7I2.38619

Parajuli, D, Vagolu, V. K., Chandramoli, K., Murali, N., & Samatha, K. (2021). Soft Chemical Synthesis of Nickel-Zinc-Cobalt-Ferrite Nanoparticles and their Structural, Morphological and Magnetic Study at Room Temperature. *Journal of Nepal Physical Society*, *7*(4), 14–18. https://doi.org/10.3126/JNPHYSSOC.V7I4.42926

Parajuli, Deependra, & Samatha, K. (2021). Structural analysis of Cu substituted Ni\Zn in Ni-Zn Ferrite. *BIBECHANA*, *18*(1), 128–133. https://doi.org/10.3126/BIBECHANA.V18I1.29475

Parajuli, Deependra, & Samatha, K. (2022). Topological properties of MXenes. In *MXenes and their Composites*. Elsevier. https://doi.org/10.1016/B978-0-12-823361-0.00015-0

Poljanšek, I., & Krajnc, M. (2005). Poljanšek and Krajnc Characterization of Phenol-Formaldehyde Prepolymer Resins. *Acta Chim. Slov*, *52*, 238–244.

Qu, C., Zhang, H., Zhang, F., & Liu, B. (2012). A high-performance anion exchange membrane based on bi-guanidinium bridged polysilsesquioxane for alkaline fuel cell application. *Journal of Materials Chemistry*, *22*(17), 8203–8207. https://doi.org/10.1039/C2JM16211C

Ran, J., Wu, L., He, Y., Yang, Z., Wang, Y., Jiang, C., Ge, L., Bakangura, E., & Xu, T. (2017). Ion exchange membranes:

New developments and applications. *Journal of Membrane Science*, *522*, 267–291. https://doi.org/10.1016/J.MEMSCI.2016.09.033

Sajjad, S. D., Liu, D., Wei, Z., Sakri, S., Shen, Y., Hong, Y., & Liu, F. (2015). Guanidinium based blend anion exchange membranes for direct methanol alkaline fuel cells (DMAFCs). *Journal of Power Sources*, *300*, 95–103. https://doi.org/10.1016/J.JPOWSOUR.2015.08.002

Sata, T. (2002). Ion Exchange Membranes Preparation, Characterization, Modification and Application. ثبثبثب, ث ققثق(ثق ثقثقثق), 314 https://books.google.com/books/about/Ion_Exchange_Membranes.html?id=QIzRdn0lGFUC

Shah, D. K., KC, D., Parajuli, D., Akhtar, M. S., Kim, C. Y., & Yang, O.-B. (2022). A computational study of carrier lifetime, doping concentration, and thickness of window layer for GaAs solar cell based on Al2O3 antireflection layer. *Solar Energy*, *234*, 330–337. https://doi.org/10.1016/J.SOLENER.2022.02.006

Shim, Y., & Kim, H. J. (2010). Nanoporous carbon supercapacitors in an ionic liquid: A computer simulation study. *ACS Nano*, *4*(4), 2345–2355. https://doi.org/10.1021/NN901916M/ASSET/IMAGES/MEDIUM/NN-2009-01916M_0009.GIF

Tuan, C. M., & Kim, D. (2016). Anion-exchange membranes based on poly(arylene ether ketone) with pendant quaternary ammonium groups for alkaline fuel cell application. *Journal of Membrane Science*, *511*, 143–150. https://doi.org/10.1016/J.MEMSCI.2016.03.059

Walker, M., Baumgärtner, K. M., Feichtinger, J., Kaiser, M., Räuchle, E., & Kerres, J. (1999). Barrier properties of plasma-polymerized thin films. *Surface and Coatings Technology*, *116–119*, 996–1000. https://doi.org/10.1016/S0257-8972(99)00216-9

Wang, T., Sun, F., Wang, H., Yang, S., & Fan, L. (2012). Preparation and properties of pore-filling membranes based on sulfonated copolyimides and porous polyimide matrix. *Polymer*, *53*(15), 3154–3162. https://doi.org/10.1016/J.POLYMER.2012.05.049

Wang, Y., & Xu, T. (2013). Ion Exchange Membranes. *Encyclopedia of Membrane Science and Technology*, 1–58. https://doi.org/10.1002/9781118522318.EMST005

Yanshan, L., Shujun, W., Hongyan, L., Fanbin, M., Huanqing, M., & Wangang, Z. (2014). Preparation and characterization of melamine/formaldehyde/polyethylene glycol crosslinking copolymers as solid–solid phase change materials. *Solar Energy Materials and Solar Cells*, *127*, 92–97. https://doi.org/10.1016/J.SOLMAT.2014.04.013

Zhang, Q., Li, S., & Zhang, S. (2010). A novel guanidinium grafted poly(aryl ether sulfone) for high-performance hydroxide exchange membranes. *Chemical Communications*, *46*(40), 7495–7497. https://doi.org/10.1039/C0CC01834A

Zheng, J., Zhang, Q., Qian, H., Xue, B., Li, S., & Zhang, S. (2017). Self-assembly prepared anion exchange membranes with high alkaline stability and organic solvent resistance. *Journal of Membrane Science*, *522*, 159–167. https://doi.org/10.1016/J.MEMSCI.2016.09.021